

Self-interacting scalar dark matter with local Z_3 symmetry

P. Ko and Yong Tang

*School of Physics,
Korea Institute for Advanced Study,
Seoul 130-722, Korea*

(Dated: March 4, 2014)

Abstract

We construct a self-interacting scalar dark matter (DM) model with local discrete Z_3 symmetry that stabilizes a weak scale scalar dark matter X . The model assumes a hidden sector with a local $U(1)_X$ dark gauge symmetry, which is broken spontaneously into Z_3 subgroup by nonzero VEV of dark Higgs field ϕ_X ($\langle\phi_X\rangle \neq 0$). Compared with global Z_3 DM models, the local Z_3 model has two new extra fields: a dark gauge field Z' and a dark Higgs field ϕ (a remnant of the $U(1)_X$ breaking). After imposing various constraints including the upper bounds on the spin-independent direct detection cross section and thermal relic density, we find that the scalar DM with mass less than 125 GeV is allowed in the local Z_3 model, in contrary to the global Z_3 model. This is due to new channels in the DM pair annihilations open into Z' and ϕ in the local Z_3 model. Most parts of the newly open DM mass region can be probed by XENON1T and other similar future experiments. Also if ϕ is light enough (a few MeV $\lesssim m_\phi \lesssim \mathcal{O}(100)$ MeV), it can generate a right size of DM self-interaction and explain the astrophysical small scale structure anomalies. This would lead to exotic decays of Higgs boson into a pair of dark Higgs bosons, which could be tested at LHC and ILC.

Keywords:

I. INTRODUCTION

Although Planck [1] has already given the dark matter(DM) relic density $\Omega h^2 = 0.1199 \pm 0.0027$ with a high precision, we still do not know particle physics nature of DM at all. So far all the compelling evidences for the existence of DM come from astrophysics and cosmology, due to its gravitational interaction. Still, many particle physics models for DMs have been proposed, and most of them have a stable collisionless cold DM(CCDM) candidate whose self-interaction can be ignored.

The collisionless cold DM has been very successful when explaining the large scale structure of our Universe. However, anomalies from the small scale astrophysical observations [2–4] indicate that DM may have strong interactions between themselves. Such self-interaction [5] would make DM have a flat core density profile rather than a cusp one predicted by CCDM. Recent simulations show that in order to flatten the cores of galaxies the cross section for DM scattering should be around $\sigma \sim M_X \times \text{barn GeV}^{-1}$ [6–8], which is in fact a huge cross section compared with typical weak-scale cross sections $\sigma \sim 10^{-12}$ barn or 1 pb. Some light particle mediator in the dark sector could be an origin of such strong self-interaction between DMs.

In this paper, we propose a scalar DM model with a local Z_3 symmetry. Unlike models based on global symmetries, local discrete symmetries can protect symmetry-breaking from quantum gravity effects and guarantee the longevity or absolute stability of DM particles. Also a light mediator can exist in the models with local symmetry, and generate the correct self-interaction for DM in explaining the anomalies mentioned in the previous paragraph.

The outline of this paper is as follows. In Sec. II, we introduce the model with a local Z_3 symmetry, establish the convention for parameters and give the physical mass spectra. Then we discuss both theoretical and experimental constraints on the parameters in Sec. III. Then in Sec. IV, we discuss the relic density and DM direct searches, paying attentions to the semi-annihilation feature, and compare with the global Z_3 mode. In Sec. V, we show that a light scalar mediator in our model can induce strong interaction for DM. Finally we summarize the results in Sec. VI.

II. LOCAL Z_3 MODEL

Let us assume the dark sector has a local $U(1)_X$ gauge which is spontaneously broken into local Z_3 symmetry a la Krauss and Wilczek [9] (see ref. [10] for local Z_N case). This can be achieved with two complex scalar fields

$$\phi_X \equiv (\phi_R + i\phi_I)/\sqrt{2}, \quad X \equiv (X_R + iX_I)/\sqrt{2}$$

in the dark sector with the $U(1)_X$ charges equal to 1 and 1/3, respectively. Then one can write down renormalizable Lagrangian for the SM fields and the dark sector fields, \tilde{X}_μ, ϕ_X and X :

$$\begin{aligned} \mathcal{L} = & \mathcal{L}_{\text{SM}} - \frac{1}{4} \tilde{X}_{\mu\nu} \tilde{X}^{\mu\nu} - \frac{1}{2} \sin \epsilon \tilde{X}_{\mu\nu} \tilde{B}^{\mu\nu} + D_\mu \phi_X^\dagger D^\mu \phi_X + D_\mu X^\dagger D^\mu X - V \\ V = & -\mu_H^2 H^\dagger H + \lambda_H (H^\dagger H)^2 - \mu_\phi^2 \phi_X^\dagger \phi_X + \lambda_\phi (\phi_X^\dagger \phi_X)^2 + \mu_X^2 X^\dagger X + \lambda_X (X^\dagger X)^2 \\ & + \lambda_{\phi H} \phi_X^\dagger \phi_X H^\dagger H + \lambda_{\phi X} X^\dagger X \phi_X^\dagger \phi_X + \lambda_{HX} X^\dagger X H^\dagger H + \left(\lambda_3 X^3 \phi_X^\dagger + H.c. \right) \end{aligned} \quad (2.1)$$

where the covariant derivative associated with the gauge field X^μ is defined as $D_\mu \equiv \partial_\mu - i\tilde{g}_X Q_X \tilde{X}_\mu$. The coupling λ_3 can be chosen as real and positive since it is always possible to redefine X to absorb the phase.

We are interested in the phase with the following vacuum expectation values for the scalar fields in the model:

$$\langle H \rangle = \frac{1}{\sqrt{2}} \begin{pmatrix} 0 \\ v_h \end{pmatrix}, \quad \langle \phi_X \rangle = \frac{v_\phi}{\sqrt{2}}, \quad \langle X \rangle = 0, \quad (2.2)$$

where only H and ϕ_X have non-zero vacuum expectation values (vev). This vacuum will break electroweak symmetry into $U(1)_{\text{em}}$, and $U(1)_X$ symmetry into local Z_3 , which stabilizes the scalar field X and make it DM. The discrete gauge Z_3 symmetry stabilizes the scalar DM even if we consider higher dimensional nonrenormalizable operators which are invariant under $U(1)_X$. This is in sharp contrast with the global Z_3 model considered in Ref. [11]. Also the particle contents in local and global Z_3 models are different so that the resulting DM phenomenology are distinctly different from each other.

Other vacuum configurations could exist, such as $\langle \phi_X \rangle \neq 0$ and $\langle X \rangle \neq 0$ which give rise to both broken $U(1)_X$ and Z_3 but also no dark matter candidate. The complete analysis of vacuum structure is beyond the scope of this work and we shall focus on the vacuum Eq. (2.2) in this paper.

Expanding the scalar fields around Eq. (2.2),

$$H \rightarrow \frac{v_h + h}{\sqrt{2}}, \quad \phi_X \rightarrow \frac{v_\phi + \phi}{\sqrt{2}}, \quad X \rightarrow \frac{x}{\sqrt{2}} e^{i\theta} \text{ or } \frac{1}{\sqrt{2}} (X_R + iX_I), \quad (2.3)$$

the minimum conditions for the potential would give

$$\left. \frac{\partial V}{\partial \phi} \right|_{x=0} = \phi \left(-\mu_\phi^2 + \lambda_\phi \phi^2 + \frac{1}{2} \lambda_{\phi H} h^2 \right) = 0, \quad (2.4)$$

$$\left. \frac{\partial V}{\partial h} \right|_{x=0} = h \left(-\mu_H^2 + \lambda_H h^2 + \frac{1}{2} \lambda_{\phi H} \phi^2 \right) = 0. \quad (2.5)$$

Then one can solve them for the VEVs as follows:

$$\langle H^2 \rangle = \frac{v_h^2}{2} = \frac{2\lambda_\phi \mu_H^2 - \lambda_{\phi H} \mu_\phi^2}{4\lambda_H \lambda_\phi - \lambda_{\phi H}^2}, \quad (2.6)$$

$$\langle \phi_X^2 \rangle = \frac{v_\phi^2}{2} = \frac{2\lambda_H \mu_\phi^2 - \lambda_{\phi H} \mu_H^2}{4\lambda_H \lambda_\phi - \lambda_{\phi H}^2}, \quad (2.7)$$

The mass matrix for the two mixed scalars is

$$\mathcal{M}^2 = \begin{pmatrix} 2\lambda_H v_h^2 & \lambda_{\phi H} v_h v_\phi \\ \lambda_{\phi H} v_h v_\phi & 2\lambda_\phi v_\phi^2 \end{pmatrix} \quad (2.8)$$

in the (h, ϕ) basis. Diagonalizing the mass matrix gives the mass eigenstates H_1 and H_2

$$\begin{pmatrix} H_1 \\ H_2 \end{pmatrix} = \begin{pmatrix} \cos \alpha & -\sin \alpha \\ \sin \alpha & \cos \alpha \end{pmatrix} \begin{pmatrix} h \\ \phi \end{pmatrix} \quad (2.9)$$

and the mixing angle

$$\tan 2\alpha = \frac{2\mathcal{M}_{12}^2}{\mathcal{M}_{22}^2 - \mathcal{M}_{11}^2} = \frac{\lambda_{\phi H} v_h v_\phi}{\lambda_\phi v_\phi^2 - \lambda_H v_h^2}, \text{ or } \sin 2\alpha = \frac{2\lambda_{\phi H} v_h v_\phi}{M_{H_2}^2 - M_{H_1}^2}.$$

Physical masses for H_1 and H_2 are

$$M_{H_1, H_2}^2 = \lambda_H v_h^2 + \lambda_\phi v_\phi^2 \pm \sqrt{(\lambda_H v_h^2 - \lambda_\phi v_\phi^2)^2 + (\lambda_{\phi H} v_h v_\phi)^2}. \quad (2.10)$$

We shall identify H_1 as the recent discovered Higgs boson with $M_{H_1} \simeq 125\text{GeV}$ and treat M_{H_2} as a free parameter. H_2 could be either heavier or lighter than H_1 . The mass for the scalar DM X is

$$M_X^2 = \mu_X^2 + \lambda_{\phi X} \frac{v_\phi^2}{2} + \lambda_{HX} \frac{v_h^2}{2}.$$

After the EW and dark gauge symmetry breaking, the mass terms for gauge fields are derived from

$$\frac{v_\phi^2}{2} \tilde{g}_X^2 \tilde{X}^\mu \tilde{X}_\mu + \frac{v_h^2}{8} \left(g_1 \tilde{B}_\mu - g_2 \tilde{W}_{3\mu} \right)^2. \quad (2.11)$$

We can redefine the abelian gauge fields

$$\begin{pmatrix} \tilde{B}_\mu \\ \tilde{X}_\mu \end{pmatrix} = \begin{pmatrix} 1 & -\tan \epsilon \\ 0 & 1/\cos \epsilon \end{pmatrix} \begin{pmatrix} \hat{B}_\mu \\ \hat{X}_\mu \end{pmatrix}, \quad \tilde{W}_\mu = \hat{W}_\mu, \quad (2.12)$$

in order to remove the kinetic mixing term between \hat{B}_μ and \hat{X}_μ . We may also rescale the gauge coupling $\hat{g}_X = \tilde{g}_X / \cos \epsilon$. Substituting with the hatted field gives the mass matrix for \hat{B} , \hat{W}_3 and \hat{X} , which we can diagonalize by rotating

$$\begin{pmatrix} \hat{B}_\mu \\ \hat{W}_{3\mu} \\ \hat{X}_\mu \end{pmatrix} = \begin{pmatrix} c_{\tilde{W}} & -s_{\tilde{W}} c_\xi & s_{\tilde{W}} s_\xi \\ s_{\tilde{W}} & c_{\tilde{W}} c_\xi & -c_{\tilde{W}} s_\xi \\ 0 & s_\xi & c_\xi \end{pmatrix} \begin{pmatrix} A_\mu \\ Z_\mu \\ Z'_\mu \end{pmatrix}. \quad (2.13)$$

Then the final mixing matrix for the starting fields in the lagrangian is

$$\begin{pmatrix} \tilde{B}_\mu \\ \tilde{W}_{3\mu} \\ \tilde{X}_\mu \end{pmatrix} = \begin{pmatrix} c_{\tilde{W}} & -(t_\epsilon s_\xi + s_{\tilde{W}} c_\xi) & s_{\tilde{W}} s_\xi - t_\epsilon c_\xi \\ s_{\tilde{W}} & c_{\tilde{W}} c_\xi & -c_{\tilde{W}} s_\xi \\ 0 & s_\xi / c_\epsilon & c_\xi / c_\epsilon \end{pmatrix} \begin{pmatrix} A_\mu \\ Z_\mu \\ Z'_\mu \end{pmatrix}. \quad (2.14)$$

In Eq. (2.13) and (2.14), we have defined the new parameters:

$$\begin{aligned} c_{\tilde{W}} &\equiv \cos \theta_{\tilde{W}} = \frac{g_2}{\sqrt{g_1^2 + g_2^2}}, \quad \tan 2\xi = -\frac{m_{\tilde{Z}}^2 s_{\tilde{W}} \sin 2\epsilon}{m_{\tilde{X}}^2 - m_{\tilde{Z}}^2 (c_\epsilon^2 - s_\epsilon^2 s_{\tilde{W}}^2)}, \\ t_x &\equiv \tan x, \quad c_x \equiv \cos x \text{ and } s_x \equiv \sin x \text{ for } x = \epsilon, \xi, \\ m_{\tilde{X}}^2 &= \hat{g}_X^2 v_\phi^2, \quad m_{\tilde{Z}}^2 = \frac{1}{4} (g_1^2 + g_2^2) v_h^2. \end{aligned} \quad (2.15)$$

From Eq. (2.14) we can observe that the SM particles charged under $SU(2)_L$ and/or $U(1)_Y$ now also have interaction with Z'_μ . And particles in the dark sector also have interaction with Z_μ due to the kinetic mixing between \hat{B}_μ and \hat{X}_μ .

The physical masses for four vector bosons in our model are given by

$$m_A^2 = 0, \quad (2.16)$$

$$m_W^2 = m_{\tilde{W}}^2 = \frac{1}{4}g_2^2 v_h^2, \quad (2.17)$$

$$m_Z^2 = m_{\tilde{Z}}^2 (1 + s_{\tilde{W}} t_\xi t_\epsilon), \quad (2.18)$$

$$m_{Z'}^2 = \frac{m_{\tilde{X}}^2}{c_\epsilon^2 (1 + s_{\tilde{W}} t_\xi t_\epsilon)}. \quad (2.19)$$

III. CONSTRAINTS ON λ 'S AND ϵ

The dimensionless parameters λ_i 's can not be arbitrarily large in perturbative theory. Demanding $|\lambda_i| \lesssim 4\pi$ would be sufficient for our consideration. The scale where perturbativity breaks down can be determined by the renormalization group (RG) analysis using the RG equations summarized in Appendix. Generally, $|\lambda_i| \lesssim 1$ at the TeV scale would give perturbativity up to 10^{15} GeV.

Besides the perturbativity, the potential should be bounded from below, which means at large field value the potential needs to be positive semidefinite, $V \geq 0$. In the limit of $\phi_i \rightarrow \infty$, we can neglect the quadratic terms and consider only the quartic part in the potential. Then in the case of $\lambda_3 = 0$ we have [12–14]

$$\lambda_H \geq 0, \lambda_\phi \geq 0, \lambda_X \geq 0, A_{\phi H} \equiv \lambda_{\phi H} + 2\sqrt{\lambda_\phi \lambda_H} \geq 0, \quad (3.1)$$

$$A_{\phi X} \equiv \lambda_{\phi X} + 2\sqrt{\lambda_\phi \lambda_X} \geq 0, A_{HX} \equiv \lambda_{HX} + 2\sqrt{\lambda_H \lambda_X} \geq 0, \quad (3.2)$$

$$\sqrt{\lambda_H \lambda_\phi \lambda_X} + \lambda_{\phi H} \sqrt{\lambda_X} + \lambda_{\phi X} \sqrt{\lambda_H} + \lambda_{HX} \sqrt{\lambda_\phi} + \sqrt{A_{\phi H} A_{\phi X} A_{HX}} \geq 0. \quad (3.3)$$

For general λ_3 , there is no transparent criteria for the positive semidefinite of V_4 . However we could get useful necessary conditions by using the general positive criteria for quartic polynomial. For instance, consider the direction in the field space,

$$h = 0, \phi_X = y \times x, X = \frac{x}{\sqrt{2}},$$

and substitute in the quartic potential, we have

$$V_4 = \frac{1}{4} (\lambda_\phi y^4 + \lambda_{\phi X} y^2 + 2\lambda_3 y + \lambda_X) x^4.$$

Boundness from below gives the constraints on the coefficients for any non-negative y

$$\lambda_\phi y^4 + \lambda_{\phi X} y^2 + 2\lambda_3 y + \lambda_X \geq 0,$$

of which one sufficient condition is

$$0 < \beta \equiv \frac{\lambda_{\phi X}}{\sqrt{\lambda_\phi \lambda_X}} \leq 6 \ \&\& \ \gamma \equiv \frac{2\lambda_3}{(\lambda_\phi \lambda_X^3)^{\frac{1}{4}}} > -\frac{\beta + 2}{2},$$

$$\text{or } \beta > 6 \ \&\& \ \gamma > -2\sqrt{\beta - 2}.$$

General conditions for positivity on a quartic polynomial of a single variable [15] is summarized in the Appendix B and shall be imposed in all following investigations.

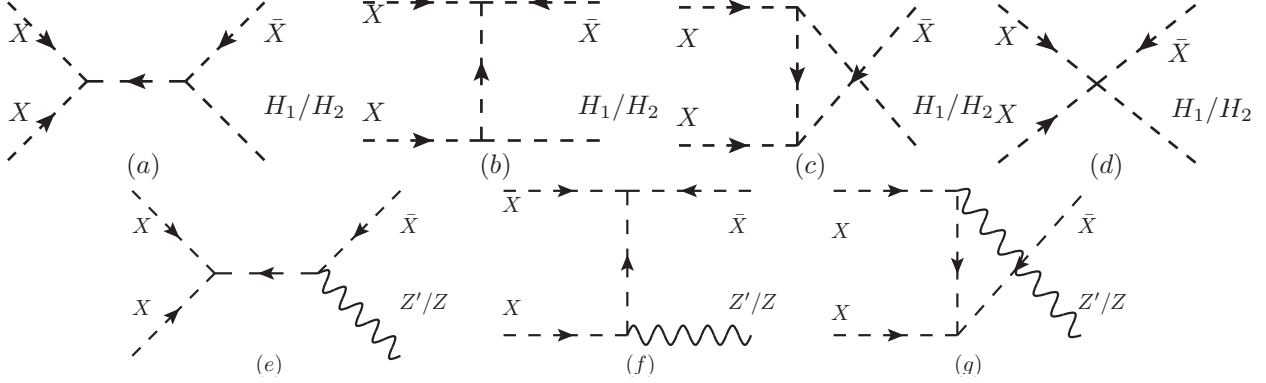


FIG. 1: Feynman diagrams for dark matter semi-annihilation. Only (a), (b), and (c) with H_1 as final state appear in the global Z_3 model, while all diagrams could contribute in local Z_3 model.

Similarly we can do the analysis in another directions. The direction $h = y \times x$, $\phi_X = 0$, $X = \frac{x}{\sqrt{2}}$ gives

$$\lambda_H y^4 + \lambda_{HX} y^2 + \lambda_X \geq 0,$$

leading constraints on λ_H , λ_X and λ_{HX} which are just those in Eq. (3.1).

Constraints on the kinetic mixing parameter ϵ come from the muon ($g-2$), atomic parity violation, the ρ parameter and electroweak precision tests (EWPTs) [16–19]. These could put an upper limit on ϵ as a function of $M_{Z'}$. Among these constraints, EWPTs provides the most stringent one:

$$\left(\frac{\tan \epsilon}{0.1}\right)^2 \left(\frac{250 \text{ GeV}}{M_{Z'}}\right)^2 \leq 0.1. \quad (3.4)$$

For $M_{Z'} \sim 250 \text{ GeV}$ we have $\epsilon \lesssim 0.03$. In the case of $\epsilon = 0$, there is no mixing between Z and Z' , the whole connection between SM and dark sector comes from the scalar sector.

In the following numerical investigation, we have imposed all the relevant constraints discussed in this section.

IV. RELIC DENSITY AND DIRECT DETECTION

A. semi-annihilation

The $X^3 \phi_X$ term and the cubic term X^3 after $U(1)_X$ symmetry breaking lend the semi-annihilation channel possible and could have a significant effect in the freeze out of the DM [20–22]. We show the relevant Feynman diagrams in Fig. 1. In the presence of semi-annihilation the Boltzman equation that determines the number density n_X is modified into [23]

$$\frac{dn_X}{dt} = -v\sigma^{XX^* \rightarrow YY} (n_X^2 - n_{X \text{ eq}}^2) - \frac{1}{2}v\sigma^{XX \rightarrow X^*Y} (n_X^2 - n_X n_{X \text{ eq}}) - 3Hn_X, \quad (4.1)$$

where Y stands for any other particles and v for the relative velocity. Due to the semi-annihilation, new contribution appears as the second term in the above equation. The

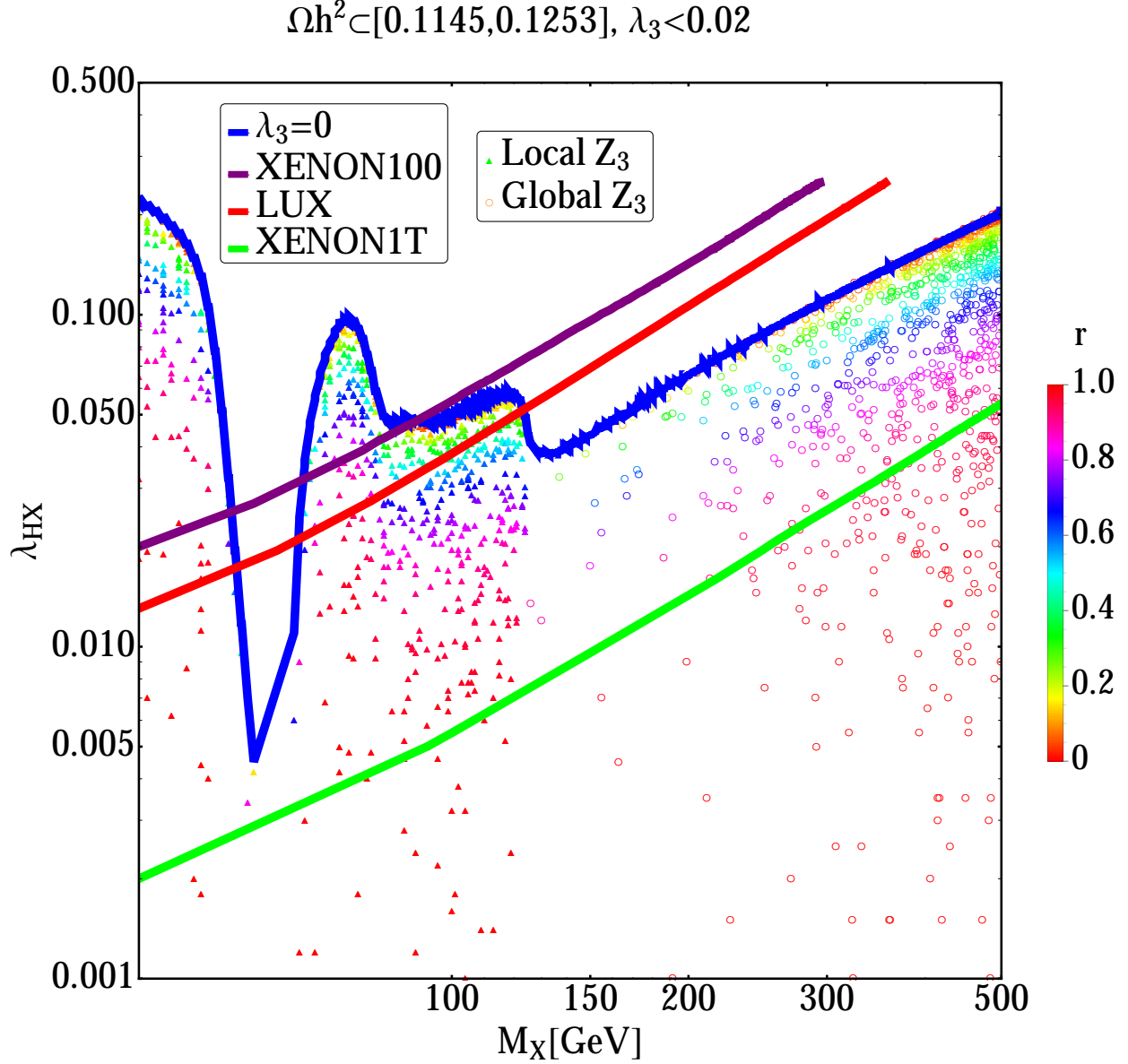


FIG. 2: Illustration of discrimination between global and local Z_3 symmetry. We have chosen $M_{H_2} = 20\text{GeV}$, $M_{Z'} = 1\text{TeV}$, $\lambda_3 < 0.02$, $\epsilon \simeq 0$ and $\lambda_{\phi H} \simeq 0$ as an example. From up to down, three nearly straight lines mark the XENON100 [24], LUX [25] and expected XENON1T limits [26], respectively. Colors in the scattered triangles and circles indicate the relative contribution of semi-annihilation, r . The curved blue band, together with the circles, gives correct relic density of X in the global Z_3 model. And the colored triangles appears only in the local Z_3 model. See text for detail.

numerical investigation is done with `micrOMEGAs` [23]. We may define the fraction of the contribution from the semi-annihilation in terms of

$$r \equiv \frac{1}{2} \frac{v\sigma^{XX \rightarrow X^*Y}}{v\sigma^{XX^* \rightarrow YY} + \frac{1}{2}v\sigma^{XX \rightarrow X^*Y}}.$$

The full Feynman diagrams for semi-annihilation are presented in Fig. 1. Depending on

the particles' masses or couplings, only a fraction of these diagrams might be kinematically allowed or relevant. For example, only first four diagram are relevant for $\epsilon \simeq 0$, $\lambda_{\phi X} \simeq 0$ and very heavy Z' . Then the cross section for $XX \rightarrow X^*H_i$ semi-annihilation process is

$$\frac{d\sigma}{d\Omega} = \frac{1}{64\pi^2 s} \frac{|p_f|}{|p_i|} |\mathcal{M}|^2,$$

with $|p_f| = \frac{1}{2\sqrt{s}} \sqrt{[s - (M_X + M_{H_i})^2][s - (M_X - M_{H_i})^2]}$. For dark matter $p_i = M_X v_{\text{vel}}/2$ and v_{vel} is the relative velocity between two annihilating particles. Matrix elements are given by

$$i\mathcal{M}_d \propto -i3\sqrt{2}\lambda_3,$$

$$i\mathcal{M}_{a+b+c} \propto -i3\sqrt{2}\lambda_3 v_\phi \left[\frac{i}{s - M_X^2} + \frac{i}{t - M_X^2} + \frac{i}{u - M_X^2} \right] (-i\lambda_{HX} v_h),$$

respectively. If $\lambda_{HX} v_h v_\phi / M_X^2 \ll 1$ and $M_{H_i} < M_X$, then \mathcal{M}_d dominates and we have

$$\langle \sigma v \rangle_d = \frac{9\lambda_3^2}{16\pi} \frac{|p_f|}{M_X^3}, \quad \text{and} \quad |p_f| \simeq \frac{3}{4}M_X \text{ for } M_X \gg M_{H_i}.$$

The relevant contribution r from semi-annihilation is shown with different color in Fig. 2. It is evident that as λ_{HX} gets smaller, r becomes larger and the semi-annihilation becomes dominant. Meanwhile the cross section for X 's scattering off a nucleon gets smaller for direct searches. Some of these points may even not be probed by XENON1T [26].

B. Global Z_3 vs Local Z_3

When the $U(1)_X$ breaking scale v_ϕ is much larger than the EW scale v_h and the masses, $M_{Z'}$ and M_{H_2} , are much heavier than those of other particles, we can get the low energy effective theory by integrating out the heavy degrees of freedom, X^μ and ϕ . The effective theory then describes the SM+ X with the residual global Z_3 symmetry. And in the effective potential the terms involving X always appears as $X^\dagger X$, X^3 and $X^{\dagger 3}$,

$$V_{\text{eff}} \simeq -\mu_H^2 H^\dagger H + \lambda_H (H^\dagger H)^2 + \mu_X^2 X^\dagger X + \lambda_X (X^\dagger X)^2 + \lambda_{HX} X^\dagger X H^\dagger H + \mu_3 X^3 + \text{higher order terms} + H.c., \quad (4.2)$$

where $\mu_3 \equiv \lambda_3 \frac{v_\phi}{\sqrt{2}}$. In such a case, the effective theory can not tell whether the Z_3 symmetry is a global one or just residual of a gauge symmetry. In fact the renormalizable parts of V_{eff} in Eq. (4.2) is exactly the same as the scalar potential in global Z_3 model [11]. Therefore we can consider the renormalizable scalar DM model with global Z_3 symmetry as an effective theory of local Z_3 models in the limit $v_\phi \gg v_h$.

However there is an important difference in the higher dimensional operators even in this limit. Within the local Z_3 model, the discrete Z_3 gauge symmetry is respected by higher dimensional operators, and the scalar DM X shall be absolutely stable. This is not the case for global Z_3 model, since the higher dimensional operators due to quantum gravity

could break global Z_3 symmetry, so that the DM stability is no longer guaranteed. For example one can consider

$$\frac{1}{\Lambda} X F_{\mu\nu} F^{\mu\nu} ,$$

which renders the scalar X with EW scale mass decay immediately, and so the scalar X cannot make a good DM candidate of the universe.

The difference between local and global Z_3 models become even more apparent and significant when $v_\phi \sim \text{TeV}$ or smaller. There is only one additional new particle X in the global Z_3 model, while in the local Z_3 model there are two more particles, Z' and H_2 , compared with the global Z_3 model. The particle spectra are different, and the local Z_3 model enjoys much richer phenomenology. In Fig. 2 we show an example that could illustrate the differences between the global and local Z_3 models. For simplicity we use $M_{H_2} = 20\text{GeV}$, $M_{Z'} = 1\text{TeV}$, $\lambda_3 < 0.02$, $\epsilon \simeq 0$ and $\lambda_{\phi H} \simeq 0$. The curved blue band shows the parameter region in which only $XX^* \rightarrow \text{SM} + \text{SM}$ processes contribute to annihilation, namely, only $\lambda_{HX} X^\dagger X H^\dagger H$ in the potential is relevant and it also marks the upper bound for λ_{HX} for giving the correct relic abundance of X in both global and local Z_3 models. We can see that the low mass range $M_X < M_{H_1}$ is excluded by latest dark matter direct search limit from LUX [25], except the resonance region $M_X \simeq M_{H_1}/2$ which will be probed by XENON1T [26]. Colored circles, together with the very curved blue band, describe the parameter space for the global Z_3 model where X^3 -term comes to play since semi-annihilation happens here only when $M_X > M_{H_1}$. However, unlike the global model, local Z_3 model allows ample parameter space in the low mass range, $M_X < M_{H_1}$, even if LUX limit is taken into account. This is shown as colored triangles in Fig. 2.

There could exist other differences between local and global Z_3 models. Depending on the exact value of $M_{Z'}$, M_{H_2} and other physical parameters, the phenomena could be quite different. For instance, when Z' or H_2 is light, H_1 can decay to them if $\epsilon \neq 0$ or $\lambda_{\phi H} \neq 0$ (see Ref. [27] for extensive survey and Ref. [28] for the comprehensive study of a singlet scalar (ϕ) mixing with the SM Higgs boson). Also, in local Z_3 model isospin-violating interaction between DM and nucleon can arise from Z' exchange. On the other hand, only isospin-conserving couplings between DM and nucleon exist in global Z_3 model through the Higgs mediation, if we neglect small isospin violation from $m_u \neq m_d$. Therefore one can have two independent channels in the DM-nucleon scattering amplitude, which might be helpful to understand the recent data on direct detection of DM in the light WIMP region [29]. This is generic in models with local dark gauge symmetry which is spontaneously broken by dark Higgs field [30].

Finally, when $M_{Z'}$ or/and M_{H_2} is about $\mathcal{O}(\text{MeV})$, sizable DM self-interaction could be realized, which is motivated to solve the astrophysical small scale structure anomalies. We shall discuss this self-interacting DM scenario in Sec. V in detail.

C. Comparison with the effective field theory (EFT) approach

In this subsection, we make a brief comparison of the renormalizable local Z_3 scalar DM model with the effective field theory (EFT) approach. Usual starting point for the EFT approach is to write down the operators for direct detections of DMs. For a complex scalar DM X we are considering in this work, one can easily construct the following operators

imposing Z_3 symmetry, to list only a few:

$$U(1)_X \text{ sym : } X^\dagger X H^\dagger H, \frac{1}{\Lambda^2} (X^\dagger D_\mu X) (H^\dagger D^\mu H), \frac{1}{\Lambda^2} (X^\dagger D_\mu X) (\bar{f} \gamma^\mu f), \text{ etc.} \quad (4.3)$$

$$Z_3 \text{ sym : } \frac{1}{\Lambda} X^3 H^\dagger H, \frac{1}{\Lambda^2} X^3 \bar{f} f, \text{ etc.} \quad (4.4)$$

$$(\text{or } \frac{1}{\Lambda^3} X^3 \bar{f}_L H f_R, \text{ if we imposed the full SM gauge symmetry}) \quad (4.5)$$

where f is a SM fermion field and Λ is a combination of new physics scale and couplings of the DM particle to new physics particle, and can differ from one operator to another. The usual story within the EFT is that the direct detection cross section due to the renormalizable operator $X^\dagger X H^\dagger H$ is strongly constrained so that the scalar DM can not be thermalized if it is light.

Note that within the EFT picture there is no room for Z' or $H_2 (\approx \phi)$ to enter and play important roles in direct and indirect detection or in the calculation of DM thermal relic density. This is because we do not know which fields are relevant (or dynamical) at the energy scale we are considering. Without constructing a full theory which is mathematically consistent and physically sensible, it would be difficult to guess which fields would be relevant beforehand within the EFT approach.

Also note that the usual complementarity does not work in this Z_3 models, since the EFT approach for direct detection based on Eq. (4.3) does not capture the semi-annihilation channels for thermal relic density or indirect DM signatures described by Eqs. (4.4) and (4.5), which is unique in the Z_3 models. This simple example shows that the DM EFT can be useful only if we know the detailed quantum numbers of DM particle, such as its spin and other (conserved) quantum numbers. Otherwise the complementarity does not work. Since we do not know anything about the DM quantum numbers as of now, the EFT approach and complementarity arguments should be taken with a great caution. Otherwise one would make erroneous conclusions.

More detailed discussions on the subtleties and limitations of EFT approach for DM physics will be discussed elsewhere [31].

V. SELF-INTERACTING DARK MATTER X

One more difference between local and global Z_3 models is that there can exist strong self-interaction between scalar DM X in the local Z_3 model¹. Traditional collisionless cold dark matter (CDM) can explain the large scale structure of the Universe. However, astrophysical anomalies in small scale structures motivate collisional CDM, which has self-interaction around $\sigma/M_X \sim 0.1 - 10 \text{ cm}^2/\text{g}$. This can be achieved in the local Z_3 model with $\mathcal{O}(\text{MeV})$ H_2 or Z' . A vector Z' can mediate both attractive and repulsive forces, and has been considered in [33–41]. So here we shall only concentrate on the $\mathcal{O}(\text{MeV})$ H_2 case in which only attractive force is mediated for explanation of small scale structures. Other different phenomenologies of a light mediator can be found in [42–50].

¹ This feature is not unique to local Z_3 model, but could appear in many other DM models with dark gauge symmetries. Another example with local Z_2 symmetry will be presented elsewhere [30].

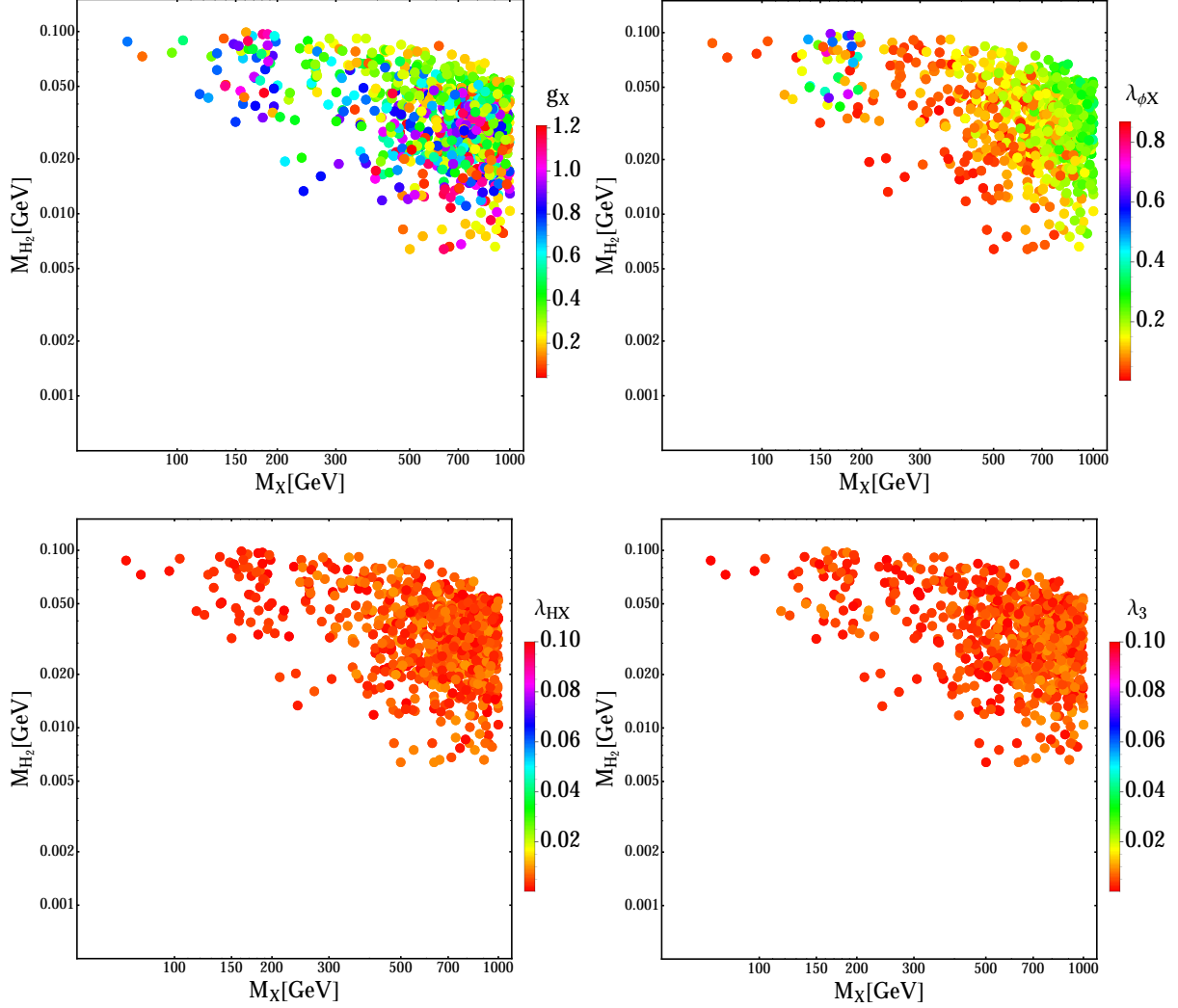


FIG. 3: Scatter plots of various parameters that are consistent with relic density, LUX direct search bound and self-interaction $\sigma_T/M_X \in [0.1, 10] \text{ cm}^2/\text{g}$ at Dwarf galaxies scale with $v_{\text{rel}} \simeq 10 \text{ km/s}$, and $\sigma_T/M_X \lesssim 0.5 \text{ cm}^2/\text{g}$ at Milky Way and cluster scales with $v_{\text{rel}} \simeq 220 \text{ km/s}$ and $v_{\text{rel}} \simeq 1000 \text{ km/s}$, respectively. We have used $M_{Z'} \simeq 200 \text{ GeV}$ and $\epsilon \ll 0.03$ and scanned other parameters as illustration.

Consider the $XX^* \rightarrow XX^*$ elastic scattering process mediated by a t-channel scalar H_2 , the differential cross section is

$$\frac{d\sigma}{d\Omega} = \frac{1}{64\pi^2 s} \frac{|p_f|}{|p_i|} |\mathcal{M}|^2, \quad \mathcal{M} \propto \frac{\lambda_{\phi X}^2 v_\phi^2}{(p_1 - p_3)^2 - M_{H_2}^2},$$

$$(p_1 - p_3)^2 = 2M_X^2 - 2(E_1 E_3 - \vec{p}_1 \cdot \vec{p}_3) = -2|\vec{p}_1|^2 (1 - \cos \theta).$$

Since $|p_f| = |p_i|$, $s \simeq 4M_X^2$, $E_1 = E_3$ and $|\vec{p}_1| = |\vec{p}_3|$ in the centre-of-mass system, then we have

$$\sigma_{\text{SI}} = \int d\Omega \frac{d\sigma}{d\Omega} = \frac{\lambda_{\phi X}^4 v_\phi^4}{64\pi M_X^2} \frac{1}{M_{H_2}^2 (4|\vec{p}_1|^2 + M_{H_2}^2)} \simeq \frac{\lambda_{\phi X}^4 v_\phi^4}{64\pi M_X^2} \frac{1}{M_{H_2}^4}, \quad \text{for } |\vec{p}_1| \ll M_{H_2}. \quad (5.1)$$

The more relevant quantity for quantifying the self-interaction of DMs is the momentum-transfer or transport cross section²

$$\sigma_T \equiv \int d\Omega (1 - \cos \theta) \frac{d\sigma}{d\Omega},$$

which regularizes the forward scattering($\theta = 0$) at which no momentum is transferred. In our case, we have for $XX^* \rightarrow XX^*$ scattering

$$\sigma_T = \frac{\lambda_{\phi X}^4 v_\phi^4}{32\pi M_X^2} \left(\frac{1}{4|\vec{p}_1|^2} \right)^2 \left[\ln(1 + R^2) - \frac{R^2}{1 + R^2} \right], \text{ where } R^2 = \frac{4|\vec{p}_1|^2}{M_{H_2}^2}. \quad (5.2)$$

This formula is consistent with [33] where a vector mediator is considered. We may rewrite the above equation as

$$\sigma_T = \frac{2\pi}{M_{H_2}^2} \beta^2 \left[\ln(1 + R^2) - \frac{R^2}{1 + R^2} \right], \text{ where } \alpha_\phi \equiv \frac{\lambda_{\phi X}^2}{4\pi} \left(\frac{v_\phi}{2M_X} \right)^2 \text{ and } \beta \equiv \frac{2\alpha_\phi M_{H_2}}{M_X v_{\text{rel}}^2}.$$

On the other hand, annihilation cross section for $XX^* \rightarrow \phi\phi$ at the freezing out time is approximately

$$\sigma_{\text{ann}} \simeq \frac{\lambda_{\phi X}^4 v_\phi^4}{64\pi M_X^2} \frac{3}{M_X^4},$$

which is much suppressed by $M_{H_2}^4/M_X^4$, compared with Eq.s (5.1) and (5.2). Naive estimates suffice to show that if we have $\sigma_{\text{ann}} \sim O(1)$ pb for $M_X \sim O(1)$ GeV, then $M_{H_2} \sim O(1) - O(100)$ MeV would give $\sigma_{\text{SI}} \sim O(1)$ barn and $\sigma_T/M_X \sim 1$ cm²/g, although more delicate analysis would involve the velocity-averaged $\langle \sigma_T \rangle$ and non-perturbative effects when $\alpha_\phi M_X > M_{H_2}$.

As an illustration, we show the scatter plots for M_{H_2} - M_X . Since we focus on the light H_2 here, we can fix $M_{Z'} = 200$ GeV and impose the constrain from electroweak precision observable, $\epsilon \ll 0.03$. Other parameters are scanned as indicated from the legend bar of individual plot.

$$g_X \lesssim 1.2, \lambda_{\phi X} \lesssim 1, \lambda_{HX} \lesssim 0.1, \lambda_3 \lesssim 0.1, \text{ and } \lambda_{\phi H} \simeq 0.$$

Because of the velocity-dependent behavior of Eq. 5.1 and 5.2, the transfer cross section over mass, σ_T/M_X , can be around $[0.1, 10]$ cm²/g at Dwarf scale with $v_{\text{rel}} \simeq 10$ km/s while still satisfy the requirement $\sigma_T/M_X \lesssim 0.5$ cm²/g to be consistent with ellipticity constraints on Milky Way and cluster scales.

Before closing this section, we briefly discuss the CMB constraints which are quite strong. When $\alpha_\phi M_X > M_\phi$, there would exist large non-perturbative effect in the low-velocity limit ($v \rightarrow 0$) of DM particle, known as Sommerfeld enhancement, and there could be relevant astrophysical constraint from cosmic microwave background(CMB) for some parameter space we discussed above. Then XX^* annihilation is enhanced at CMB time and significant energy would be injected to photon-baryon bath, broadening the last scattering surface and

² If the scattering particles are identical, $XX \rightarrow XX$ for instance, it may be more appropriate to use the $\sigma_T \equiv \int d\Omega (1 - \cos^2 \theta) \frac{d\sigma}{d\Omega}$ which regularizes both forward and backward scattering [32].

leaving an imprint in CMB spectra [51–58]. Current data constrains the enhancement factor $S \lesssim \mathcal{O}(1000)$ for $\mathcal{O}(\text{TeV})$ DM with the exact value depending on the specific annihilation channel. As an illustration, taking parameters for large self-interactions for the DM’s such as

$$M_X \simeq 1\text{TeV}, M_\phi \simeq 1\text{MeV}, \lambda_{\phi X} \simeq 0.1,$$

we find that the enhancement factor saturates at $S \sim \mathcal{O}(50)$, which is well below the current limit, $S \lesssim \mathcal{O}(1000)$. Therefore the discussions on self-interacting DM presented in this section are safe from the CMB constraints.

Finally let us add that this mechanism for enhancing the DM self-interactions could be realized not only by light scalar mediator ϕ but also by a light vector mediator Z' between X and X^* (namely, between opposite dark charges). Thus this feature is not unique to local Z_3 models, and could be easily realized in other models too, such as local Z_2 models [30].

VI. SUMMARY

In this paper, we have proposed a self-interacting scalar DM model with a local dark Z_3 symmetry. Unlike global dark symmetries, local ones can guarantee that DM is absolutely stable even in the presence of higher dimensional nonrenormalizable operators due to the underlying local gauge symmetry. Then we discussed perturbativity constraints on the scalar potential and the experimental limit on the kinetic mixing. Compared with a global Z_3 model, our scenario has two new particles, Z' and H_2 , and there are new channels in the DM pair annihilations for thermalizing DMs. Therefore much ampler parameter space is allowed including a light DM with $M_X < 125$ GeV, most region of which can be probed with future DM direct searches. Also, motivated by the small scale astrophysical anomalies, we investigated the phenomenology of a MeV scalar H_2 in our model which has no counterpart in the minimal global Z_3 model. Thanks to the velocity dependence of DM self-interaction cross section, such a light H_2 can mediate strong interaction for DM scattering at Dwarf galaxy scale while satisfying Milky Way and cluster scale constraints. Similar arguments go for the light Z' as well. For such a light H_2 or Z' , there could be exotic decays of the 126 GeV Higgs boson, which could be studied in the upcoming LHC running and at future lepton colliders.

Acknowledgments

We are grateful to Seungwon Baek and Wan-Il Park for useful comments and discussions. This work is supported in part by National Research Foundation of Korea (NRF) Research Grant 2012R1A2A1A01006053 (PK,YT), and by the NRF grant funded by the Korea government (MSIP) (No. 2009-0083526) through Korea Neutrino Research Center at Seoul National University (PK).

VII. APPENDIX

A. RGEs

For future reference, here we present the RGEs in the case of no kinetic mixing,

$$\begin{aligned}
\frac{d\lambda_H}{d\ln\mu} &= \frac{1}{16\pi^2} \left[24\lambda_H^2 + \lambda_{\phi H}^2 + \lambda_{HX}^2 - 6y_t^4 + \frac{3}{8} \left(2g_2^4 + (g_1^2 + g_2^2)^2 \right) - \lambda_H (9g_2^2 + 3g_1^2 - 12y_t^2) \right], \\
\frac{d\lambda_\phi}{d\ln\mu} &= \frac{1}{16\pi^2} \left[20\lambda_\phi^2 + 2\lambda_{\phi H}^2 + \lambda_{\phi X}^2 + 6g_X^4 - 12\lambda_\phi g_X^2 \right], \\
\frac{d\lambda_X}{d\ln\mu} &= \frac{1}{16\pi^2} \left[20\lambda_X^2 + 2\lambda_{HX}^2 + \lambda_{\phi X}^2 + 9\lambda_3^2 + \frac{2}{27}g_X^4 - \frac{4}{3}\lambda_\phi g_X^2 \right], \\
\frac{d\lambda_{\phi H}}{d\ln\mu} &= \frac{1}{16\pi^2} \left[4\lambda_{\phi H} (3\lambda_H + 2\lambda_\phi + \lambda_{\phi H}) + \lambda_{\phi X} \lambda_{HX} - \lambda_{\phi H} \left(\frac{9}{2}g_2^2 + \frac{3}{2}g_1^2 - 6y_t^2 + 6g_X^2 \right) \right], \\
\frac{d\lambda_{HX}}{d\ln\mu} &= \frac{1}{16\pi^2} \left[4\lambda_{HX} (3\lambda_H + 2\lambda_X + \lambda_{HX}) + \lambda_{\phi H} \lambda_{\phi X} - \lambda_{HX} \left(\frac{9}{2}g_2^2 + \frac{3}{2}g_1^2 - 6y_t^2 + \frac{2}{3}g_X^2 \right) \right], \\
\frac{d\lambda_{\phi X}}{d\ln\mu} &= \frac{1}{16\pi^2} \left[2\lambda_{\phi X} (2\lambda_\phi + 2\lambda_X + \lambda_{\phi X}) + 2\lambda_{\phi H} \lambda_{HX} + 18\lambda_3^2 - \lambda_{HX} \left(6g_X^2 + \frac{2}{3}g_X^2 \right) \right], \\
\frac{dg_X}{d\ln\mu} &= \frac{1}{16\pi^2} \left(\frac{1}{3} + \frac{1}{27} \right) g_X^3, \\
\frac{d\lambda_3}{d\ln\mu} &= \frac{1}{16\pi^2} [\lambda_3 (2\lambda_X + \lambda_{\phi X})].
\end{aligned}$$

B. Positive Conditions for Quartic Polynomial

This section summarizes the positivity conditions for quartic polynomials, see Ref.[15] for mathematical details. For a general quartic polynomial

$$f(z) = az^4 + bz^3 + cz^2 + dz + e, \quad (7.1)$$

with real coefficients, positive a and e , $f(z) \geq 0$ for $z > 0$ shall constrain the regions of coefficients. Positivity on any fixed interval (u, v) can be translated directly to positivity on the positive reals through the transformation

$$t = \frac{u + zv}{1 + z}.$$

With the replacement $x^4 = \frac{a}{e}z^4$, the polynomial $f(z)/e$ then becomes $p(x) = x^4 + \alpha x^3 + \beta x^2 + \gamma x + 1$, where we have defined

$$\alpha = ba^{-\frac{3}{4}}e^{-\frac{1}{4}}, \beta = ca^{-\frac{1}{2}}e^{-\frac{1}{2}}, \gamma = da^{-\frac{1}{4}}e^{-\frac{3}{4}}.$$

Now the question is shifted to the positivity of $p(x)$ for $x \geq 0$. Define

$$\Delta = 4[\beta^2 - 3\alpha\gamma + 12]^3 - [72\beta + 9\alpha\beta\gamma - 2\beta^3 - 27\alpha^2 - 27\gamma^2]^2, \quad (7.2)$$

$$\Lambda_1 \equiv (\alpha - \gamma)^2 - 16(\alpha + \beta + \gamma + 2), \quad (7.3)$$

$$\Lambda_2 \equiv (\alpha - \gamma)^2 - \frac{4(\beta + 2)}{\sqrt{\beta - 2}} \left(\alpha + \gamma + 4\sqrt{\beta - 2} \right). \quad (7.4)$$

Then $p(x) \geq 0$ for all $x \geq 0$ or $f(z) \geq 0$ for all $z > 0$ if and only if

$$(1) \beta < -2 \text{ and } \Delta \leq 0 \text{ and } \alpha + \gamma > 0; \quad (7.5)$$

$$(2) -2 \leq \beta \leq 6 \text{ and } \begin{cases} \Delta \leq 0 & \text{and } \alpha + \gamma > 0 \\ \Delta \geq 0 & \text{and } \Lambda_1 \leq 0; \end{cases} \quad (7.6)$$

$$(3) 6 < \beta \text{ and } \begin{cases} \Delta \leq 0 & \text{and } \alpha + \gamma > 0 \\ \alpha > 0 & \text{and } \gamma > 0 \\ \Delta \geq 0 & \text{and } \Lambda_2 \leq 0. \end{cases} \quad (7.7)$$

It is also useful to give the following sufficient conditions for positivity,

$$(1) \alpha > -\frac{\beta+2}{2} \text{ and } \gamma > -\frac{\beta+2}{2} \text{ for } \beta \leq 6, \quad (7.8)$$

$$(2) \alpha > -2\sqrt{\beta-2} \text{ and } \gamma > -2\sqrt{\beta-2} \text{ for } \beta > 6. \quad (7.9)$$

-
- [1] P. A. R. Ade *et al.* [Planck Collaboration], arXiv:1303.5076 [astro-ph.CO].
 - [2] S. -H. Oh, W. J. G. de Blok, E. Brinks, F. Walter and R. C. Kennicutt, Jr, arXiv:1011.0899 [astro-ph.CO].
 - [3] M. Boylan-Kolchin, J. S. Bullock and M. Kaplinghat, Mon. Not. Roy. Astron. Soc. **415**, L40 (2011) [arXiv:1103.0007 [astro-ph.CO]].
 - [4] M. Boylan-Kolchin, J. S. Bullock and M. Kaplinghat, Mon. Not. Roy. Astron. Soc. **422**, 1203 (2012) [arXiv:1111.2048 [astro-ph.CO]].
 - [5] D. N. Spergel and P. J. Steinhardt, Phys. Rev. Lett. **84**, 3760 (2000) [astro-ph/9909386].
 - [6] M. Vogelsberger, J. Zavala and A. Loeb, Mon. Not. Roy. Astron. Soc. **423**, 3740 (2012) [arXiv:1201.5892 [astro-ph.CO]].
 - [7] M. Rocha, A. H. G. Peter, J. S. Bullock, M. Kaplinghat, S. Garrison-Kimmel, J. Onorbe and L. A. Moustakas, Mon. Not. Roy. Astron. Soc. **430**, 81 (2013) [arXiv:1208.3025 [astro-ph.CO]].
 - [8] J. Zavala, M. Vogelsberger and M. G. Walker, Monthly Notices of the Royal Astronomical Society: Letters **431**, L20 (2013) [arXiv:1211.6426 [astro-ph.CO]].
 - [9] L. M. Krauss and F. Wilczek, Phys. Rev. Lett. **62** (1989) 1221.
 - [10] B. Batell, Phys. Rev. D **83** (2011) 035006 [arXiv:1007.0045 [hep-ph]].
 - [11] G. Belanger, K. Kannike, A. Pukhov and M. Raidal, JCAP **1301**, 022 (2013) [arXiv:1211.1014 [hep-ph]].
 - [12] K. Hadeler. 1983. On copositive matrices. Linear Algebra Appl.,49,79
 - [13] G. Chang and T. W. Sederberg. Nonnegative quadratic Bzier triangular patches, Computer Aided Geometric Design 11 (1994), no. 1 113 - 116.
 - [14] K. Kannike, Eur. Phys. J. C **72**, 2093 (2012) [arXiv:1205.3781 [hep-ph]].
 - [15] Gary Ulrich, Layne T. Watson, "Positivity conditions for quartic polynomials", Siam Journal on Scientific Computing 01/1994; 15(3):528-544, DOI:10.1137/0915035.
 - [16] J. Kumar and J. D. Wells, Phys. Rev. D **74** (2006) 115017 [hep-ph/0606183].
 - [17] W. -F. Chang, J. N. Ng and J. M. S. Wu, Phys. Rev. D **74** (2006) 095005 [Erratum-ibid. D **79** (2009) 039902] [hep-ph/0608068].
 - [18] P. Fayet, Phys. Rev. D **75** (2007) 115017 [hep-ph/0702176 [HEP-PH]].

- [19] E. J. Chun, J. -C. Park and S. Scopel, JHEP **1102**, 100 (2011) [arXiv:1011.3300 [hep-ph]].
- [20] T. Hambye, JHEP **0901**, 028 (2009) [arXiv:0811.0172 [hep-ph]].
- [21] F. D’Eramo and J. Thaler, JHEP **1006** (2010) 109 [arXiv:1003.5912 [hep-ph]].
- [22] G. Belanger, K. Kannike, A. Pukhov and M. Raidal, JCAP **1204** (2012) 010 [arXiv:1202.2962 [hep-ph]].
- [23] G. Belanger, F. Boudjema, A. Pukhov and A. Semenov, arXiv:1305.0237 [hep-ph].
- [24] E. Aprile *et al.* [XENON100 Collaboration], Phys. Rev. Lett. **109**, 181301 (2012) [arXiv:1207.5988 [astro-ph.CO]].
- [25] D. S. Akerib *et al.* [LUX Collaboration], arXiv:1310.8214 [astro-ph.CO].
- [26] E. Aprile [XENON1T Collaboration], arXiv:1206.6288 [astro-ph.IM].
- [27] D. Curtin, R. Essig, S. Gori, P. Jaiswal, A. Katz, T. Liu, Z. Liu and D. McKeen *et al.*, arXiv:1312.4992 [hep-ph].
- [28] S. Choi, S. Jung and P. Ko, JHEP **1310**, 225 (2013) [arXiv:1307.3948].
- [29] G. v. Blanger, A. Goudelis, J. -C. Park and A. Pukhov, JCAP **1402**, 020 (2014) [arXiv:1311.0022 [hep-ph]].
- [30] S. Baek, P. Ko and W.I. Park, in preparation.
- [31] Work in progress.
- [32] J. M. Cline, Z. Liu, G. Moore and W. Xue, arXiv:1311.6468 [hep-ph].
- [33] J. L. Feng, M. Kaplinghat and H. -B. Yu, Phys. Rev. Lett. **104** (2010) 151301 [arXiv:0911.0422 [hep-ph]].
- [34] M. R. Buckley and P. J. Fox, Phys. Rev. D **81** (2010) 083522 [arXiv:0911.3898 [hep-ph]].
- [35] A. Loeb and N. Weiner, Phys. Rev. Lett. **106**, 171302 (2011) [arXiv:1011.6374 [astro-ph.CO]].
- [36] L. G. van den Aarssen, T. Bringmann and C. Pfrommer, Phys. Rev. Lett. **109**, 231301 (2012) [arXiv:1205.5809 [astro-ph.CO]].
- [37] S. Tulin, H. -B. Yu and K. M. Zurek, Phys. Rev. Lett. **110**, 11, 111301 (2013) [arXiv:1210.0900 [hep-ph]].
- [38] S. Tulin, H. -B. Yu and K. M. Zurek, Phys. Rev. D **87**, 115007 (2013) [arXiv:1302.3898 [hep-ph]].
- [39] S. Hannestad, R. S. Hansen and T. Tram, Phys. Rev. Lett. **112** (2014) 031802 [arXiv:1310.5926 [astro-ph.CO]].
- [40] B. Dasgupta and J. Kopp, Phys. Rev. Lett. **112** (2014) 031803 [arXiv:1310.6337 [hep-ph]].
- [41] T. Bringmann, J. Hasenkamp and J. Kersten, arXiv:1312.4947 [hep-ph].
- [42] M. Pospelov, A. Ritz and M. B. Voloshin, Phys. Lett. B **662** (2008) 53 [arXiv:0711.4866 [hep-ph]].
- [43] D. Hooper and K. M. Zurek, Phys. Rev. D **77** (2008) 087302 [arXiv:0801.3686 [hep-ph]].
- [44] J. L. Feng and J. Kumar, Phys. Rev. Lett. **101** (2008) 231301 [arXiv:0803.4196 [hep-ph]].
- [45] J. L. Feng, H. Tu and H. -B. Yu, JCAP **0810** (2008) 043 [arXiv:0808.2318 [hep-ph]].
- [46] N. Arkani-Hamed, D. P. Finkbeiner, T. R. Slatyer and N. Weiner, Phys. Rev. D **79** (2009) 015014 [arXiv:0810.0713 [hep-ph]].
- [47] M. Pospelov and A. Ritz, Phys. Lett. B **671** (2009) 391 [arXiv:0810.1502 [hep-ph]].
- [48] W. Shepherd, T. M. P. Tait and G. Zaharijas, Phys. Rev. D **79** (2009) 055022 [arXiv:0901.2125 [hep-ph]].
- [49] D. E. Kaplan, M. A. Luty and K. M. Zurek, Phys. Rev. D **79** (2009) 115016 [arXiv:0901.4117 [hep-ph]].
- [50] H. An, S. -L. Chen, R. N. Mohapatra and Y. Zhang, JHEP **1003** (2010) 124 [arXiv:0911.4463 [hep-ph]].

- [51] S. Galli, F. Iocco, G. Bertone and A. Melchiorri, Phys. Rev. D **80**, 023505 (2009) [arXiv:0905.0003 [astro-ph.CO]].
- [52] T. R. Slatyer, N. Padmanabhan and D. P. Finkbeiner, Phys. Rev. D **80**, 043526 (2009) [arXiv:0906.1197 [astro-ph.CO]].
- [53] M. Cirelli, F. Iocco and P. Panci, JCAP **0910**, 009 (2009) [arXiv:0907.0719 [astro-ph.CO]].
- [54] G. Hutsi, J. Chluba, A. Hektor and M. Raidal, Astron. Astrophys. **535** (2011) A26 [arXiv:1103.2766 [astro-ph.CO]].
- [55] A. Natarajan, Phys. Rev. D **85** (2012) 083517 [arXiv:1201.3939 [astro-ph.CO]].
- [56] J. M. Cline and P. Scott, JCAP **1303**, 044 (2013) [Erratum-ibid. **1305**, E01 (2013)] [arXiv:1301.5908 [astro-ph.CO]].
- [57] R. Diamanti, L. Lopez-Honorez, O. Mena, S. Palomares-Ruiz and A. C. Vincent, JCAP02(2014)017 [arXiv:1308.2578 [astro-ph.CO]].
- [58] M. S. Madhavacheril, N. Sehgal and T. R. Slatyer, arXiv:1310.3815 [astro-ph.CO].